Scheduling and feed quality optimization of concentrate raw materials in the copper refining industry

Yingkai Song[†], *Brenno C. Menezes*[†], *Pablo Garcia-Herreros*[§], *Ignacio E. Grossmann*[†*]

[†] Department of Chemical Engineering. Carnegie Mellon University. Pittsburgh, PA 15213, USA.

§ Research, Development & Innovation. Aurubis AG. Hamburg, Germany.

ABSTRACT

The scheduling and feed quality optimization for processing solid concentrates in the copper refining industry is formulated as a large-scale discrete time non-convex Mixed-Integer Non-Linear Program (MINLP) that includes logistics operations and ad-hoc blending constraints. For this complex problem, the full space MINLP for the blending of concentrates and the scheduling of the logistics is partitioned into a Mixed-Integer Linear Program (MILP) and in a Non-Linear Program (NLP). The solution strategy considers the relax-and-fix rolling horizon with nearby time window overlaps and the use of multiple MILP solutions to be applied in a two-step MILP-NLP procedure. Two models are proposed for the flowsheet balances: a split fraction model and a process network model. The results indicate that the split fraction model yields near optimal solutions with a large computational effort, while the process network can generate several feasible solutions faster. We present a motivating example and an industrial problem with MILP to NLP gaps close to 0%.

1. Introduction

Copper is one of the most important metals in industry because of inherent properties: high thermal and electrical conductivity, good corrosion resistance, malleability, among others.[1] With the widespread evolution of the internet of things and the brand-new projects on smart cities, the demand of copper for telecommunications, energy supply, and traffic infrastructures, is expected to increase. Among other applications, copper plays an important role in the development of electric vehicles. According to a research conducted by IDTechEx [2], the battery of an electric vehicle has 83 kg of copper, which is more than 3.5 times the content of an internal combustion engine. Consequently, copper demand for electric vehicles is expected to increase from 185,000 tons in 2017 to 1.74 million tons in 2027. Renewable energy generation technologies, such as wind, ocean and solar installations are also copper intensive[3]. The installation of 1 MW of offshore wind energy requires about 6 tons of copper; a photovoltaic plant requires about 4 tons/MW, appreciably more than an oil-fired power plant (1.1 tons/MW) or a nuclear power plant (0.7 tons/MW).

Given the current and future importance of copper, this work proposes a methodology to optimize the scheduling and feed-mix blending of concentrates in a copper refinery, with the purpose of improving the operational results based on an economic metric. The final product of the process is copper cathodes, a high purity sheet of copper that can be sold as a commodity. The typical process of transforming copper concentrates into copper cathodes can be divided into three stages: smelting, converting and electrorefining. These processes transform the raw materials into a final product containing more than 99.99% copper.[1]

Since copper concentrates with diverse composition are obtained from ores widespread over the world, the procurement of concentrates is an important decision-making challenge. In addition, many quality restrictions apply to the chemical composition of the concentrates because of the conditions required for smelting and other steps of the refining process. Therefore, an enterprise-wide optimization approach integrating the scheduling and feed blending operations in the processing site can lead to high-performance production since the smelter and downstream units are very sensitive the composition of the raw materials. For this reason, a blend scheduling optimization model can unveil the potential value of complex quality feeds.

To the best of our knowledge, there is no research work reported on scheduling and feed quality optimization in the copper processing industry. Nevertheless, we can find similarities with the crude-oil blend scheduling problem: both processes integrate batch, semi-continuous, and continuous operations as blending and scheduling are executed considering logistic and quality constraints. Therefore, similar modeling and solution strategies can be used to tackle the blending and scheduling problems of both crude-oils and copper concentrates, despite the difference arising from operating with solid materials instead of liquids. As described in the next sections, several logistics constraints must be considered to transport, store, and mix copper concentrates.

The blend scheduling optimization of copper concentrates involving its logistics and quality aspects in a given topology is a challenging problem since it gives rise to a complex MINLP model. To optimize such systems of raw materials, Lee et al.[4] developed a first approach for scheduling in crude-oil refineries based on a discrete-time formulation. The MINLP model is reformulated as an MILP problem by relaxing the bilinear terms representing the blending quality constraints, which can lead to streams with different component concentration leaving the same quality tank. Mendez et al.[5] proposed a sequential MILP approach to simultaneously solve the blending and scheduling optimization of petroleum fuels using an approximation that successively updates a delta (the difference between the linear and nonlinear blending correlations) to iteratively correct the MILP blending predictions.

However, the main strategy in the literature of blending and scheduling optimization to consider several stages of storage, mixing, and movement of raw materials involved in the logistics and feed quality operations, is to decompose the MINLP model into the solution of MILP and NLP programs.[6-11] In such MILP-NLP decomposition approach, the quality information from the mixing of streams is neglected in the MILP step, which might produce infeasibilities in the NLP subproblems if the discrete assignments found in the MILP do not allow matching the quality constraints of the NLP. Alternatives in the literature to approximate the non-linearities of blending in the MILP before solving the NLPs make use of: a) piecewise McCormick envelopes to linearly under- and over-estimate the bilinear terms,[12-15] b) multiparametric disaggregation,[7] and c) augmented equality balances as cuts of quality material flows.[16] Successive substitution to iteratively correct the MILP predictions[5,16] have also been used to start the NLPs.

In terms of the time representation, despite the advances in MILP solvers, the simultaneous blending and scheduling optimization in both continuous- and discrete-time formulations have moved away the efforts from the latter to the more compact continuous-time approaches.[6-10,17,18] Strengths and weaknesses of discrete- and continuous-time formulations have been summarized by Joly and Pinto[19] and Floudas and Lin.[20] Broadly speaking, discrete-time models are faster and easier to understand, and ultimately to implement at the operating/process level. However, the time intervals must be sufficiently short to properly represent the blending and scheduling problems. Although the discrete-time models present a tighter LP relaxation, the solution of industrial problems may demand strategies such as Benders[21] or Lagrangean[22] decomposition, or some sort of rolling-horizon techniques integrated with a relax-and-fix method for the discrete decisions.[15,23,24] On the other hand, continuous-time formulations can be easily solved for several types of problems since a smaller number of discrete decision are required. Major drawbacks are in the weaker LP relaxation and possible solutions including very small-time intervals which cannot be executed in practice. In addition, manpower bottlenecks can be a barrier to execute the scheduling in a specific point in time of the continuous-time rather than in a time-step window as in the discrete-time model. Lee and Maravelias[25] proposed a hybrid modeling of time by combining continuous-time in a refined discrete-time approach that can bring new alternative to scheduling problems.

Further to the discussion on MINLP solution strategies and the time representation, a major topic concerning the proposed blending and scheduling optimization problem is the modeling of the quantity and quality balances in the blending or pooling locations. Misener and Floudas[26] present a comprehensive survey on modeling and optimization of the pooling problem. The main two formulations are: a) the *p*-formulation by Haverly[27] based on total flows and composition variables, which is widely used in chemical industry and b) the *q*-formulation by Ben-Tal et al.[28] that keeps track of the proportion of raw materials in the flows, which often performs better with branch-and-cut algorithms.[29] Sahinidis and Tawarmalani[30] also presented a *pq*-formulation producing a tighter relaxation for the pooling problem by adding two particular constraint sets to the q-formulation.

Recently, Lotero et al.[31] formulated the source based (SB) model which is similar to the split fraction (SF) model proposed by Quesada and Grossmann,[32] although the sources are tracked instead of the specifications. In the (SF) model, the fraction of specification *q* in a stream is defined as the amount of flow of specification *q* in the stream divided by the total flow between tanks (see eq. 3b). In the (SB) model, the composition of a stream is determined from the compositions of each of the sources present in the stream. More details about the difference between models can be found in Lotero et al.[31]

We propose two alternative formulations for the discrete-time multiperiod blend scheduling problem of copper concentrates: the multiperiod process network formulation that derives from the standard *p*-formulation and the multiperiod split fraction formulation that derives from the split fraction model proposed by Quesada and Grossmann[32], which is similar but not identical to the *q*-formulation.

The remaining of this article is organized as follows. In section 2, the problem statement of the blend scheduling of copper concentrates is explained. In section 3, the split fraction and process network formulations for modeling the mass and quality balances in the problem are presented, as well as the binary relations for specific logistics operations and quality constraints in terms of composition of elements. In section 4, solution strategies to solve the decomposed MILP are presented, namely the relax-and-fix rolling horizon scheme using time blocks with time-step overlapping and the generation of multiple binary solutions. Finally, computational results are presented to show the effectiveness of the proposed solution strategy and the performance of the split fraction and process network models. Both, the motivating example and the industrial problem are modeled using the two different formulations.

2. The raw material blend scheduling problem

The raw material blend scheduling problem in this article considers the arrivals of maritime vessels containing solid copper concentrates. These raw materials are initially unloaded at the maritime port, where the different copper concentrates are separately piled in preparation for the first mixing step (see Figure 1). The mixed concentrates are loaded in transfer ships and dispatched to the processing facility through a river transportation system. These pre-blends are received at the production facility to be directly fed into several bins of the smelter furnace. Daily arrival of non-concentrate materials are also added to the bins in lower amounts.

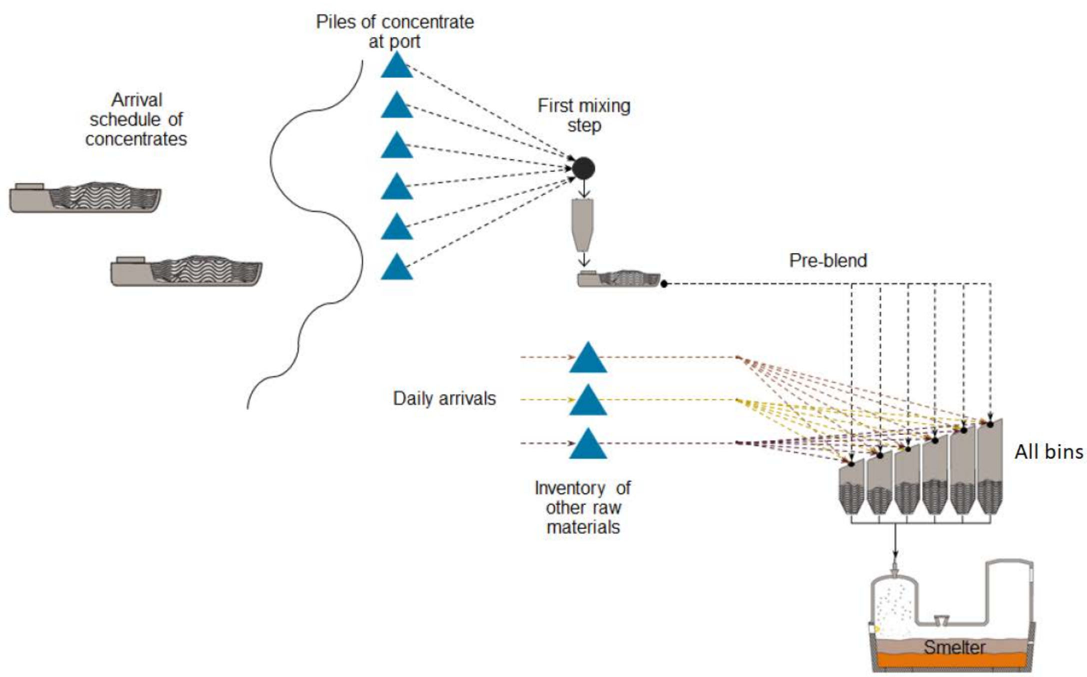

Figure 1. Topology of the blend scheduling network for the copper refining plant

Similar to the final quality constraints in blending and scheduling of crude oils, there are upper bounds on the mass fraction of key components in the mixtures to be processed in the smelter. In addition, the process includes interdependency constraints based on individual key component flowrates; these constraints model restrictions for the subsequent stages in the refining process, such as the converting and electro-refining stages.[1] In such linear constraints, for example, a flowrate of K1 component would be lower than a flowrate of K2, or other linear constraints involving flowrates and other parameters can be modeled as will be shown in the industrial example.

In a crude oil blend scheduling problem[4,6], the objective function considers the gross margin for processing the raw materials and the cost of inventory management and unloading. In the proposed blending and scheduling of copper raw materials, variations in the concentration of key components in the mixture are undesirable in the smelting process due to operational stability. Therefore, penalties are also considered for variations in the concentration of certain key components in the objective function, since it provides a balance between profit and operational stability.

Complex logistic operations of intermediate units such as transfer ships and bins, are also needed for processing the copper containing raw materials. They are described in detail below.

Operation of the maritime vessels. Vessels with different types of copper concentrates arrive on the port during the time horizon. The vessels unload all the materials as piles at the expected arrival time period and it is assumed that the time period is long enough for the vessels to discharge all materials. There are unlimited capacities on the port. Inventory cost and unloading cost are neglected.

Operation of the pre-blender. The pre-blender on the port has unlimited capacity and can simultaneously receive material from several piles while it is not charging a transfer ship. Part of a pile can be sent to the pre-blender in one time period, not necessarily the whole pile. The pre-blender can also be discharged to two or more transfer ships simultaneously. The quality of mixed raw materials in the pre-blender is not under control.

Operation of the transfer ships. River cargo ships transfer the pre-blends of copper concentrates from the maritime port to the production facility. There is a cycle time for the transfer considering time of loading, transporting, unloading, and returning, which gives rise to the *transport delay*. Unloading materials from the river ships in the production facility follows a general rule: *shut down when empty*. This means that unloading operations are executed until the ships are empty. The transfer ships can be discharged into two or more bins simultaneously. Two or more transfer ships are allowed to unload materials simultaneously to different bins.

Operation of the bins. Several bins feed the smelter through conveyor belts simultaneously and continuously. One bin can only be charged by one resource at one time period, either from one transfer ship or from one pile of daily-arrival material. If a vessel arrives when all bins are being charged by difference resources, the vessel must wait to unload the materials. The bins function similarly to the charging tanks in crude oil scheduling problem but not exactly in the same way. First, a charging tank cannot be charged and discharged simultaneously, but a bin is charged and discharged simultaneously and continuously feeding the smelter throughout the time horizon. Second, all materials in a charging tank are well-blended; a bin can contain more than one feed mix or blend since there is no mechanical agitation nor blending of the solids in the bins. Therefore, a single bin can successively feed the smelter with blends having different concentrations. In the process, the smelter is charged by a continuous moving belt that transport the raw materials stored at the bins. For better control of the process, it is required that the feeding process from the bins are coordinated to start and end a given feeding recipe (or smelter diet) simultaneously. Otherwise, if one bin starts feeding the smelter with new mixtures, there might be the need to abruptly adjust another conveyor belt to satisfy quality constraints.

Operation of the sub-bins. To model the operations for the bins described above (without simultaneous charging and discharging such as a standing-gauge tank), we model each bin by dividing it into two sub-bins. The sub-bins follow the assumptions as shown below.

i. The sub-bins have unlimited capacity.

ii. Each sub-bin cannot be charged and discharged simultaneously. It can only be charged from one source at a time, either from one transfer ship or from one pile of non-concentrate material, when it is empty. Blending is forbidden in the sub-bins, i.e. a sub-bin cannot be charged by two different resources in successive time periods.

iii. The sub-bins can only start charging the smelter a few time periods after the transfer process is initiated because there are no initial inventories in the intermediate units. Based on the proposed rules of operation and the transport delay for the transfer ships, it takes time for the raw materials to reach the smelter from the port. In this particular case, the smelter can work continuously after time period 5 as shown in Figure 2.

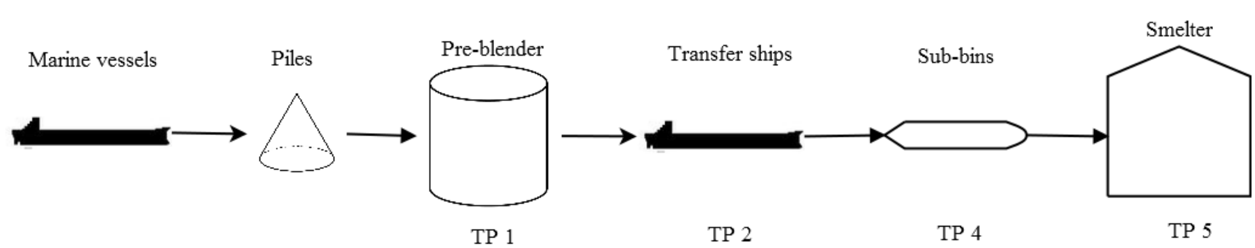

Figure 2. Time delay for the material transport

iv. The sub-bins are grouped into two pre-defined sets with only one set charging the smelter at any time t, i.e. when a group of sub-bins are feeding the smelter, the other group can be charged. In addition, every sub-bin in one working group must start to feed the smelter simultaneously and must stop feeding the smelter simultaneously. Figure 3 illustrates how this modeling scheme works.

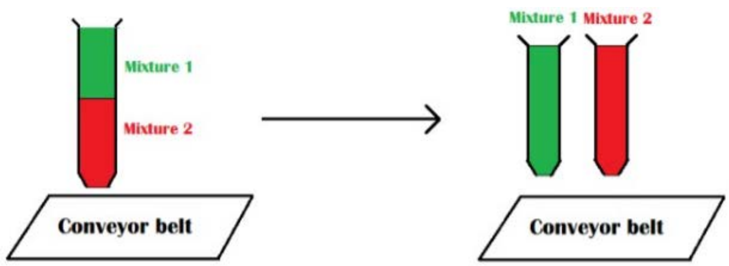

Figure 3. Modeling method: 2 sub-bins for each bin.

v. The sub-bins obey the general rule, shut down when empty, which means that a working sub-bin can be supplying material to the smelter over one or more time periods until it becomes empty. If the sub-bins of the working group become empty, a feeding blend ends and another blend can start using the other group.

Operation of the daily arrivals of non-concentrate materials. There are daily arrivals of non-concentrate materials in the production facility, which are mainly leftovers from other refining processes. It is required that the daily arrival material is not accumulated in the production facility and it must be consumed at the end of the scheduling horizon.

Operation of the smelter. The smelter must be operated continuously at full capacity.

The goal of the optimization problem is to maximize the gross margin obtained from processing raw materials, which implies determining the schedule of the operations to be executed as well as the amount of concentrates to be transferred from the port to the plant. Penalties for variation in the composition of key components are also considered. Therefore, the model aims to find the most profitable blend schedule with consideration of the logistic restrictions and the operational stability of the smelting furnace.

3. Mathematical model

The mathematical model for blending and scheduling of copper concentrates shown in Figure 4 involves quantity and quality balances, as well as operational relationships considering the resources and their connections. Figure 4 is a schematic representation of the illustrative example proposed for the scheduling and feed quality optimization problem of copper concentrates. Each bin is modeled by two sub-bins, as we shall discuss in section 3.2.5. The main resources used in the model are concentrates *c*, marine vessels *v*, piles *p*, pre-blender *b*, transfer ships *ts*, daily arrival piles *dp*, sub-bins *sb*, and the smelter *s*.

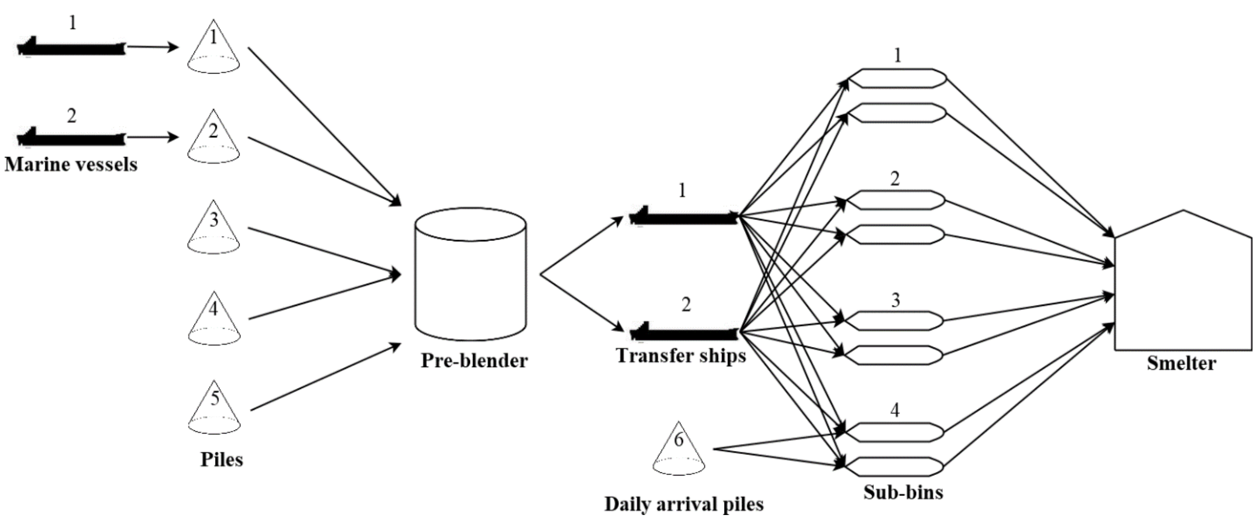

Figure 4. Schematic representation of the mixing network of the motivating example

In the problem, copper concentrates with different concentration of key components *k* are unloaded at the maritime port, and different piles *p* are formed separately. A first mixing step takes place in the pre-blending facility *b*, where the blend is loaded into the transfer ships *ts* that transport it to the processing plant. Once the transfer ships arrive to the plant, they feed the sub-bins *sb.* The final blend is the result of a second mixing step that is controlled by varying the speed of the conveyor belts connecting each sub-bin to the smelter *s*.

As mentioned earlier, we developed two alternatives to describe mathematically the flow, storage, and mixing of copper concentrates. For a unit *n*, considering upstream units $i \in I_n$ and downstream units $o \in O_n$, we formulate the models based on the following approaches:

a) A multiperiod Process Network model (PN) including raw material concentrations $x_{n,c,t}$ in total flows ($F_{i,n,t}$ or $F_{n,o,t}$) and total amounts ($M_{i,n,t}$ or $M_{n,o,t}$), derived from the standard *p*-formulation for continuous process in the Harvely pooling formulation[27];

b) A multiperiod Split Fraction model (SF) considering flow proportions of inlets *i* and outlets *o* ($f_{i,n,t}$ or $f_{n,o,t}$), derived from the split fraction model for continuous process proposed by Quesada and Grossmann[32].

3.1. Quantity and quality balances of blending and scheduling

We formulate the process network and the split fraction models for the quantity and quality balances of the blending and scheduling processes that originate at the maritime port and end at the smelter. The process network formulation includes total inventories, flow, and composition variables of each intermediate unit and stockpile; in this model, the nonlinearities arise on the blending of flows when calculating the blended material composition. Disaggregated inventories and flow variables for each type of copper concentrate are considered in the split fraction model and the bilinear terms appear when intermediate units are discharging.

3.1.1. Process network model (PN)

The process network formulation is derived from the standard *p*-formulation. The mass and quality balances in this model for a continuous process are shown in eq. 1a and eq. 1b,

$$\sum_{i \in I_n} F_{i,n} = \sum_{o \in O_n} F_{n,o} \qquad n \in N \tag{1a}$$

$$\sum_{i \in I_n} F_{i,n} x_{i,c} = \sum_{o \in O_n} F_{n,o} x_{o,c} \qquad n \in N, c \in C \tag{1b}$$

where $F_{i,n}$ represents the total inlet from unit i to the unit n and $F_{n,o}$ is the total outlet from the unit n to the unit o. $x_{i,c}$ is the mass fraction of concentrate c in unit i and $x_{o,c}$ is the mass fraction of concentrate c in the unit o.

The multiperiod process network model requires two additional equations: eq. 2a models the total mass balance of inventories; eq.2b represents inventories of individual concentrates c modeled by the total inventories $M_{n,t}$ times the composition variables $x_{n,c,t}$, which is the mass fraction of concentrate c in unit n at time t.

$$M_{n,t} = M_{n,t-1} + \sum_{i \in I_n} F_{i,n,t} - \sum_{o \in O_n} F_{n,o,t} \qquad n \in N, t \in T \tag{2a}$$

$$M_{n,t} x_{n,c,t} = M_{n,t-1} x_{n,c,t-1} + \sum_{i \in I_n} F_{i,n,t} x_{i,c,t-1} - \sum_{o \in O_n} F_{n,o,t} x_{n,c,t-1} \qquad n \in N, c \in C, t \in T \tag{2b}$$

3.1.2. Split fraction model (SF)

Quesada and Grossmann[32] proposed a split fraction model including the flow variables and inventory of different concentrates *c* and the split fraction of discharge, as shown in eq. 3a and eq. 3b.

$$\sum_{i \in I_n} f_{i,n,c} = \sum_{o \in O_n} f_{n,o,c} \qquad n \in N, c \in C \tag{3a}$$

$$\frac{\sum_{i \in I_n} f_{i,n,c}}{\sum_{i \in I_n} f_{i,n,c'}} = \frac{f_{n,o,c}}{f_{n,o,c'}} \qquad n \in N, o \in O_n, (c \neq c') \in C \tag{3b}$$

Eq. 3a is the mass balance for inlet ($f_{i,n,c}$) and outlet ($f_{n,o,c}$) flows of concentrate c going through unit *n*; eq. 3b forces the split fraction of the outlet flows to be identical to the aggregated concentrate fraction of inlet flows.

The split fraction model mentioned above is not the same as the standard *q*-formulation[28]. The split fraction model tracks exactly the specifications, which is the individual flow of concentrate *c* in the proposed blending problem instead of proportion variables. The proportion variables in the *q*-formulation[29] are the fraction of flows coming from different sources, which are the raw materials in different vessels and initial inventories at the port in the proposed blending problem.

We apply the idea of split fraction model for continuous process to the multiperiod blending problem and introduce variables for total inventories and flowrates in the stockpiles and units. The mass balances aggregating the amounts of different concentrates are shown in eq. 4a-4d.

$$M_{n,t} = \sum_{c \in C} m_{n,c,t} \qquad n \in N, t \in T \tag{4a}$$

$$F_{n,o,t} = \sum_{c \in C} f_{n,o,c,t} \qquad n \in N, o \in O_n, t \in T \tag{4b}$$

Eq. 4a correspond to the balances between total inventory variables and disaggregated inventories. Eq. 4b represents the balances between total flows and disaggregated flows. In particular, $M_{n,t}$ models the total inventory of intermediate unit *n* at time *t*; $m_{n,c,t}$ is the corresponding individual inventory of concentrate *c*; $F_{n,o,t}$ represents the total outflow of unit *n* to the downstream unit *o*; and $f_{n,o,c,t}$ is the corresponding individual outflow of concentrate c.

The individual inventory of concentrate c at time *t* is defined by adding to the individual inventory at *t*-1 all the inlet and outlet individual flowrate at time *t* as shown in eq. 4c.

$$m_{n,c,t} = m_{n,c,t-1} + \sum_{i \in I_n} f_{i,n,c,t} - \sum_{o \in O_n} f_{n,o,c,t} \qquad n \in N, c \in C, t \in T \tag{4c}$$

The composition of the products transferred during a transfer operation at *t* must be identical to the composition at the origin tank at *t*-1,

$$\frac{m_{n,c,t-1}}{M_{n,t-1}} = \frac{f_{n,o,c,t}}{F_{n,o,t}} \qquad n \in N, c \in C, o \in O_n, t \in T$$

which can be reformulated with bilinear terms according to eq. 4d.

$$m_{n,c,t-1} F_{n,o,t} = M_{n,t-1} f_{n,o,c,t} \qquad n \in N, c \in C, o \in O_n, t \in T \tag{4d}$$

The logic constraints modeling the transfer of material from unit *n* to their downstream units $o \in O_n$ are shown in constraints 5a and 5b,

$$F_{n,o,t} \geq \underline{F_{n,o}} D_{n,o,t} \qquad n \in N, o \in O_n, t \in T \tag{5a}$$

$$F_{n,o,t} \le \overline{F_{n,o}} D_{n,o,t} \qquad n \in N, o \in O_n, t \in T \qquad (5b)$$

where $[\underline{F_{n,o}}, \overline{F_{n,o}}]$ are defined as the bounds on flow from unit n to unit o, and $D_{n,o,t}$ are binary variables indicating if unit n is charging unit o at time t.

3.2. Operations for blending and scheduling of stock piles

The operation to handle the solid stock piles and flows of concentrates c are modeled with the mixed–integer constraints described below.

3.2.1. Operation of the maritime vessels

The vessels transporting copper concentrates unload all the raw material when they arrive to the port, in contrast to the crude oil tankers[4,6], which typically unload in multiple time-periods due to pipeline bottlenecks. In our model, the vessels can unload all material on the port as a pile p without considering unloading cost or storage tanks. Therefore, the vessels' operation is pre-defined. We define the parameter $F_{v,p,t}$ to indicate the flowrate from vessel v to pile p at time t.

3.2.2. Operation of the pre-blender

The pre-blender b cannot be charged and discharged simultaneously. Instead of defining binary variables for flow from piles to the pre-blender, we define binary variables $X_{b,t}$ to indicate if the pre-blender is charging any transfer ships (see Figure 5). Then, the flow from piles to the pre-blender is indicated by 1-$X_{b,t}$. $D_{b,ts,t}$ is a binary variable indicating if the pre-blender b is charging transfer ship ts at time t. The corresponding constraints are given by the inequalities 6-7.

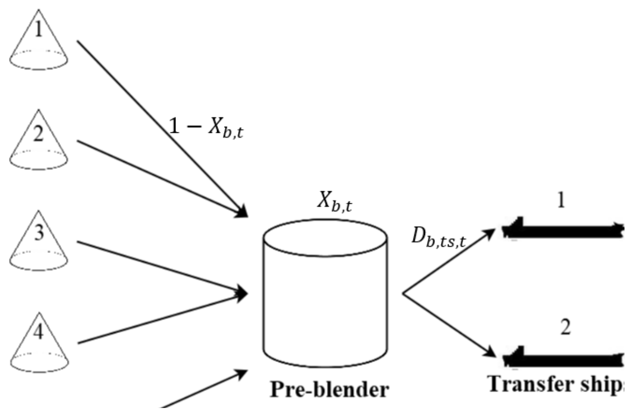

Figure 5. The method for modeling the operations of the pre-blender

If the pre-blender is charging any transfer ship ($D_{b,ts,t} = 1$), $X_{b,t}$ must be 1.

$$D_{b,ts,t} \le X_{b,t} \qquad b \in B, ts \in TS, t \in T \tag{6a}$$

If the pre-blender is not charging any transfer ship ($\sum_{ts \in TS} D_{b,ts,t} = 0$), $X_{b,t}$ must be 0.

$$\sum_{ts \in TS} D_{b,ts,t} \ge X_{b,t} \qquad b \in B, t \in T \tag{6b}$$

If the pre-blender is not charging any transfer ship ($X_{b,t} = 0$), the feeding process from piles is allowed and its flow $F_{p,b,t}$ is given by:

$$F_{p,b,t} \ge \underline{F_{p,b}}(1 - X_{b,t}) \qquad b \in B, p \in P, t \in T \tag{7a}$$

$$F_{p,b,t} \le \overline{F_{p,b}}(1 - X_{b,t}) \qquad b \in B, p \in P, t \in T \tag{7b}$$

3.2.3. Operation of the transfer ships

The operations of the transfer ships between the port and production facility consider a *transport delay,* which means that the duration time for loading, transportation, and unloading are all equal to one time period. The transfer ships should always unload all the material in the production facility, which is the *shut down when empty* condition.

The constraints for *transport delay* are given by inequalities 8a-8c.

The transfer ships cannot be charged ($D_{b,ts,t}$) and discharged ($D_{ts,sb,t}$) simultaneously,

$$D_{ts,sb,t} + D_{b,ts,t} \le 1 \qquad b \in B, ts \in TS, sb \in SB, t \in T \tag{8a}$$

where $D_{ts,sb,t}$ is defined as a binary variable to indicate if transfer ship *ts* is charging sub-bins *sb* at time *t*.

The transfer ships cannot be charged and discharged in successive time periods.

$$D_{ts,sb,t+1} + D_{b,ts,t} \le 1 \qquad b \in B, ts \in TS, sb \in SB, t \in T \tag{8b}$$

$$D_{ts,sb,t} + D_{b,ts,t+1} \le 1 \qquad b \in B, ts \in TS, sb \in SB, t \in T \tag{8c}$$

In order to model the *shut down when empty* condition for unloading operations in a single time period, we define the binary variable $E_{ts,t}$ to indicate if there are materials in transfer ship *ts* at the end of time *t*; this condition is modeled with constraints 9a and 9b.

$$M_{ts,t} \le \overline{M_{ts}} E_{ts,t} \qquad ts \in TS, t \in T \tag{9a}$$

$$M_{ts,t} \ge \underline{M_{ts}} E_{ts,t} \qquad ts \in TS, t \in T \tag{9b}$$

where $[\underline{M_{ts}}, \overline{M_{ts}}]$ are the bounds on inventories of transfer ship *ts*.

Constraints 10a-10b ensure that each transfer ship *ts* charges only one sub-bin *sb* at the same time; binary variables $X_{ts,t}$ indicate if the transfer ship *ts* is charging any sub-bin *sb* at time *t*; binary variables $D_{ts,tb,t}$, indicate if transfer ship *ts* is charging sub-bin *sb* at time t. A similar formulation was proposed by Zyngier and Kelly.[33]

$$D_{ts,sb,t} \le X_{ts,t} \qquad ts \in TS, sb \in SB, t \in T \tag{10a}$$

$$\sum_{sb \in SB} D_{ts,sb,t} \ge X_{ts,t} \qquad ts \in TS, t \in T \tag{10b}$$

The *shut down when empty* is enforced with constraints 11a and 11b. If transfer ship *ts* is unloading material at time *t* ($X_{ts,t} = 1$), it must be empty at the end of time *t* ($E_{ts,t} = 0$).

$$X_{ts,t} + E_{ts,t} \le 1 \qquad ts \in TS, t \in T \tag{11a}$$

Furthermore, if transfer ship *ts* is being charged by the pre-blender at time *t* ($\sum_{b \in B} D_{b,ts,t} = 1$), the transfer ship *ts* must be initially empty ($E_{ts,t-1} = 0$).

$$E_{ts,t-1} + \sum_{b \in B} D_{b,ts,t} \le 1 \qquad ts \in TS, t \in T \tag{11b}$$

3.2.4. Operation of the daily arrivals of non-concentrate materials

The inventory of daily arrival material should be below a certain value at the end of the time horizon. This constraint is different for the split fraction model and the process network model. Since the split fraction model has variables indicating the inventories each raw material in, the condition can be easily described with the linear constraint 12,

$$\sum_{dp \in DP} m_{dp,c,t} + \sum_{sb \in SB} m_{sb,c,t} \leq MD \qquad c \in DC, t = TMH \tag{12}$$

where $m_{dp,c,t}$ and $m_{sb,c,t}$ represent the amount of non-concentrate material c ($c \in DC$) in daily arrival pile dp and in sub-bin sb at time t, respectively. MD represents the maximum amount of this non-concentrate material in the system at the end of time horizon, TMH. The recycling and reprocessing materials c ($c \in DC$) both stocked in the daily arrival piles and in the sub-bin downstream connected to them are regarded in constraints 12 and 13.

In the process network model, bilinear terms are necessary for describing the amount of non-concentrate materials both stocked in the piles and within the sub-bins at the end of scheduling horizon. In order to propose a MILP approximation necessary for the solution strategy described in Section 4, we impose the constraints that the sub-bins should be empty at the end of scheduling horizon. These condition is modeled with constraints 13a and 13b.

$$M_{dp,t} \leq MD \qquad dp \in DP, t = TMH \tag{13a}$$

$$M_{sb,t} = 0 \qquad sb \in SB, t = TMH \tag{13b}$$

Even though the formulations of the split fraction and process network models are not equivalent, the difference does not affect the optimal solution as will be shown in the computational results section. In other words, the sub-bins with non-concentrate materials ($c \in DC$) are always empty at the end of time horizon, whether we impose eq. 13b or not.

3.2.5. Operation of the sub-bins

The purpose of the sub-bins as a modeling strategy is to force the bins to feed the same recipe simultaneously and coordinate the change-over to the next recipe. We divide all sub-bins (set

FSB and set *SSB*) into two groups containing exactly one sub-bin from every bin. For each group, we define a set of binary variables, Df_t and Ds_t, indicating if the first (Df_t) or second (Ds_t) group of sub-bins is charging the smelter at time *t*. Constraints 14a and 14b ensure that each sub-bin is either being charged with non-concentrate materials *dp*, is being charged with concentrates from the transfer ships *ts*, or is feeding the smelter.

$$\sum_{dp \in DP} D_{dp,sb,t} + Df_t + \sum_{ts \in TS} D_{ts,sb,t} \le 1 \qquad sb \in FSB, t \in T \tag{14a}$$

$$\sum_{dp \in DP} D_{dp,sb,t} + Ds_t + \sum_{ts \in TS} D_{ts,sb,t} \le 1 \qquad sb \in SSB, t \in T \tag{14b}$$

The two groups of sub-bins should work in cycles after the starting of smelting process ($t \geqslant ET$) as imposed with eq. 15.

$$Df_t + Ds_t = 1 \qquad t \ge ET \tag{15}$$

In order to model the operation *shut down when empty* of the sub-bins' feeding process in multiple time periods, we define the variable $E_{sb,t}$ to indicate if there are materials in the sub-bin *sb* at time *t* according to constraints 16a and 16b.

$$M_{sb,t} \le \overline{M_{sb}} E_{sb,t} \qquad sb \in SB, t \in T \tag{16a}$$

$$M_{sb,t} \ge \underline{M_{sb}} E_{sb,t} \qquad sb \in SB, t \in T \tag{16b}$$

New binary variables $D\hat{f}_t$ and $D\hat{s}_t$ are introduced to indicate when one feeding recipe ends as shown in Figure 6. Consider the first group of sub-bins as an example.

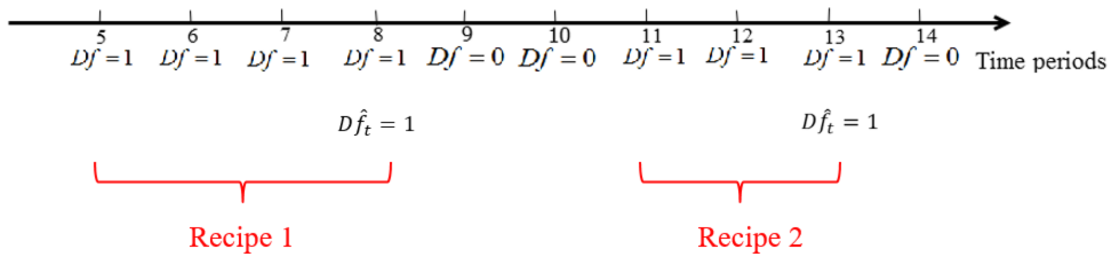

Figure 6. Binary variables indicating end of recipe.

Constraints 17a-17c model the end of a feeding recipe with variables $D\hat{f}_t$ and $D\hat{s}_t$. If one feeding recipe ends at time *t* ($D\hat{f}_t = 1$), the sub-bins must feed the smelter at time *t* ($Df_t = 1$).

$$D\hat{f}_t \le Df_t \qquad t \in T \tag{17a}$$

If one feeding recipe ends at time *t* ($D\hat{f}_t = 1$), the group of sub-bins cannot feed the smelter at time *t*+1 ($Df_{t+1} = 0$).

$$D\hat{f}_t + Df_{t+1} \le 1 \qquad t \in T \tag{17b}$$

If the sub-bins feed the smelter at time *t* ($Df_t = 1$), and do not feed the smelter at time *t*+1 ($Df_{t+1} = 0$), the group of sub-bins end a feeding recipe at time t ($D\hat{f}_t = 1$).

$$Df_{t+1} + D\hat{f}_t \ge Df_t \qquad t \in T \tag{17c}$$

The same definition is applied to $D\hat{s}_t$ as shown in constraints 18a-18c.

$$D\hat{s}_t \le Ds_t \qquad t \in T \tag{18a}$$

$$D\hat{s}_t + Ds_{t+1} \leq 1 \qquad t \in T \tag{18b}$$

$$Ds_{t+1} + D\hat{s}_t \geq Ds_t \qquad t \in T \tag{18c}$$

The *shut down when empty* condition is enforced with constraints 19a-19c.

If the sub-bins finish charging the smelter at time *t* (e.g., $D\hat{f}_t = 1$ for the first bins), then they must be empty at the end of time *t* ($E_{sb,t} = 0$).

$$D\hat{f}_t + E_{sb,t} \leq 1 \qquad sb \in FSB, t \in T \tag{19a}$$

$$D\hat{s}_t + E_{sb,t} \leq 1 \qquad sb \in SSB, t \in T \tag{19b}$$

If the sub-bin *sb* is non-empty ($E_{sb,t-1} = 1$), it cannot be charged by any of the transfer ships or daily arrival piles ($\sum_{dp \in DP} D_{dp,sb,t} + \sum_{ts \in TS} D_{ts,sb,t} = 0$).

$$\sum_{dp \in DP} D_{dp,sb,t} + \sum_{ts \in TS} D_{ts,sb,t} + E_{sb,t-1} \leq 1 \qquad sb \in SB, t \in T \tag{19c}$$

3.3. Final blending and quality constraints

The smelter works at full capacity continuously starting at *ET* and the sum of flowrate from sub-bins are equal to the maximum flowrate into the smelter, as shown in eq. 20a and eq.20b,

$$\overline{F}_t = \sum_{sb \in SB} F_{sb,s,t} \qquad t \in T \tag{20a}$$

$$\overline{F}_t = \widehat{F}_s \qquad t \geq ET \tag{20b}$$

where $\hat{F}_s$ corresponds to the full capacity of the smelter.

The conversion from concentrates total flow to the flow of individual key components $\tilde{F}_{k,t}$ is calculated based on their assay. The constraints necessary for the split fraction model are linear as shown in eq. 21. The equivalent constraints are nonlinear for the process network model as in eq. 22.

$$\tilde{F}_{k,t} = \sum_{sb \in SB} \sum_{c \in C} \sum_{s \in S} f_{sb,s,c,t} \theta_{k,c} \qquad k \in K, t \in T \tag{21}$$

$$\tilde{F}_{k,t} = \sum_{sb \in SB} \sum_{c \in C} \sum_{s \in S} F_{sb,s,t} x_{sb,c,t-1} \theta_{k,c} \qquad k \in K, t \in T \tag{22}$$

Here, $\theta_{k,c}$ is the assay describing the composition of key components *k* in concentrate *c*, and $x_{sb,c,t-1}$ represents the mass fraction of concentrate *c* at time *t*-1.

Quality constraints. We specify an upper bound for the mass fraction of key components, χ_k in the final blending.

$$\bar{F}_t \chi_k \geq \tilde{F}_{k,t} \qquad k \in K, t \in T \tag{23}$$

Interdependency constraints. The constraints model complex quality restrictions that relate the content of different key components in the blends. Equations 24a-24c are based on individual flows, where *kk* is alias of *k*. Ue_k and Ke_k are the parameters related to the interdependency constraints.

$$0.64 \tilde{F}_{k2,t} \geq \tilde{F}_{k7,t} \qquad t \in T \tag{24a}$$

$$0.58\tilde{F}_{k2,t} \leq \tilde{F}_{k7,t} \qquad t \in T \tag{24b}$$

$$Ue_k \sum_{kk \in K} (Ke_{kk} \tilde{F}_{kk,t}) \geq Ke_k \tilde{F}_{k,t} \qquad k \in K, t \in T \tag{24c}$$

3.4. Objective function

The objective is to maximize the gross margin of processing different kinds of raw materials, while considering penalties for the variation in concentration of key components. The objective function for both split fraction model (SF) and the process network model (PN) have the same physical interpretation; however, their formulations are different. Eq. 25 presents the linear objective function for the split fraction model (SF). The nonlinear objective function of the process network model is presented in eq. 26.

$$\max \sum_{t \in T} \sum_{sb \in SB} \sum_{s \in S} \sum_{c \in C} f_{sb,s,c,t} \alpha_c - \sum_{t \in T} \sum_{k \in K} Z_{k,t} \beta_k \tag{25}$$

$$\max \sum_{t \in T} \sum_{sb \in SB} \sum_{s \in S} \sum_{c \in C} F_{sb,s,t} x_{sb,c,t-1} \alpha_c - \sum_{t \in T} \sum_{k \in K} Z_{k,t} \beta_k \tag{26}$$

Here, α_c is defined as the income for processing unit concentrate *c*, while β_k is the pre-defined weight of flow change for key component k. The positive variables $Z_{k,t}$, defining the flow change for key component *k*, is defined according to eq. 27a and 27b.

$$Z_{k,t} \geq \tilde{F}_{k,t} - \tilde{F}_{k,t-1} \qquad k \in K, t \in T \tag{27a}$$

$$Z_{k,t} \geq \tilde{F}_{k,t-1} - \tilde{F}_{k,t} \qquad k \in K, t \in T \tag{27b}$$

4. Solution strategy

4.1. Solution strategy for split fraction model

4.1.1. MILP-NLP decomposition method

Theoretically, the nonconvex MINLP model can be solved using any global solver such as BARON or a local optimal solver such as DICOPT. However, because of the high nonlinearity and large size of the model, BARON can be prohibitively expensive to use, while DICOPT may converge to poor suboptimal solutions. Therefore, a two-step procedure is proposed that leads to local optimal solutions with an estimation of the optimality gap. In the first step, an MILP relaxation of the model without the nonlinear constraints (4d), is solved using CPLEX. In the second step, the nonlinear constraints are enforced, and all binary variables are fixed, which means the schedule of operations is fixed. The resulting nonlinear programming model is solved using the solution of the MILP as a starting point by a global NLP solver, BARON or local NLP solver CONOPT. The solution at this stage may not correspond to the global optimum of the model in the full space or may even be infeasible. However, the optimality gap can be estimated from the solution of the MILP and the feasible NLP. If the NLP returns an objective value identical to the MILP's, then global optimality is proven. As shown in the computational results section, near-optimal solutions are obtained in which the MILP-NLP gap is close to zero.

4.1.2. Relax-and-fix rolling horizon with nearby time window overlaps

The MILP model of the motivating example in a split fraction model can be solved by CPLEX in the full space considering all binary variables are simultaneously calculated. However, for the industrial problem in a split fraction model, the first MILP model cannot be solved in reasonable solution time since the size of industrial problem is too large. Therefore, a *relax-and-fix rolling horizon with nearby time window overlaps* method is proposed to solve this large scale MILP model. A rolling horizon algorithm is applied similar to the production-distribution coordination of crude-oil scheduling presented by Assis et al.[15] and industrial gases supply chains presented by Zamarripa et al.[23] The rolling horizon method divides the time horizon into a *detailed time block* where binary variables are considered and an *aggregate time block* where binary variables are relaxed to 0-1 continuous variables; the method successively solves a set of subproblems in which discrete decisions are fixed in previous time periods, as shown in Figure 7.

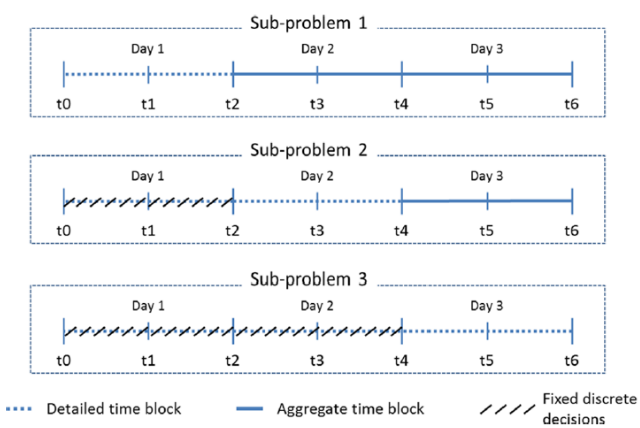

Figure 7. The illustrative example of rolling horizon by Zamarripa et al (2016)

However, considering that in this raw material blending problem we have special operation rules, the rolling horizon mentioned above can lead to infeasible solutions after fixing binary decisions in the previous time block; this can lead to infeasible problem in subsequent sub-problems. Therefore, a rolling horizon strategy with relaxation overlaps is applied in this work. We have overlapping time periods for the binary relaxations between the aggregate time block and the next detailed time block to avoid infeasible solutions in the solution process.

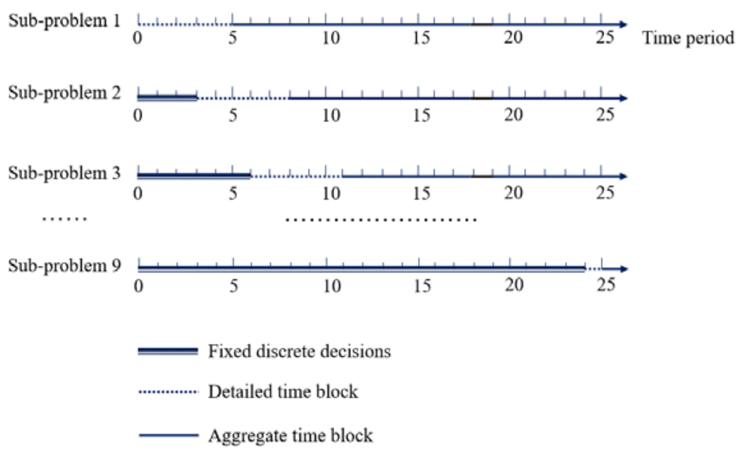

Figure 8. Proposed rolling horizon with relaxation overlapping for the illustrative example.

The scheme presented in Figure 8 shows an illustrative example in which we describe a problem with 25 time periods. We have 9 subproblems solved sequentially. Subproblem 1: time periods 1-5 are considered as the detailed time block, while the rest time periods are considered as the aggregate time block. Subproblem 2: Even though the solution from time period 1-5 is known, we only fix the binary variables of time period 1-3, which means the overlap between the first and second detailed time block is 2 time periods. Then the detailed time block of subproblem 2 is from 4-8. This procedure is repeated until the last subproblem in which there is only one detailed time block to the end of the scheduling horizon.

Theoretically, the objective value by this rolling horizon with overlap method is always lower than the one obtained by solving the full space. However, the suitable combination of the length of the detailed time block and overlap can reduce the gap between the solution by this strategy and the global optimal solution. There is trade-off between the lengths of the detailed time block and overlap periods, and the computational result. If the detailed time block and overlap are longer, it will require a large computational effort, but the solution can be expected to be closer to the optimal solution from solving the full space model. If the detailed time block is shorter, the computational effort is smaller, but the solution might be further away from the optimal solution, and there is a higher potential for infeasible solutions. Since the length of the detailed time blocks and overlaps need to be postulated before running the rolling horizon with the relaxation overlapping algorithm, we have tested different combinations of the length of detailed time blocks and overlaps and select the best combination to obtain the best objective value with relatively less computational effort. We applied this rolling horizon with overlap strategy to the MILP of the industrial problem as shown in the computational results section.

4.2. Solution strategy for process network model

4.2.1. MILP-NLP decomposition method

The MILP-NLP decomposition algorithm is also applied to the process network model but with some differences. For the split fraction model, the objective functions of the MILP and NLP are the same, which is the gross margin minus the penalties of variation in feed concentration. However, in the process network model, once we drop the nonlinear eq. 2b and 26 in the MILP, there is one total flow throughout the flowsheet and the composition information is no longer available, which means that it is not possible to estimate the gross margin in the first MILP model. To overcome this problem, we substitute the objective function shown eq.26 by eq. 28, which maximizes the total flowrate into the smelter during the scheduling horizon.

$$\max \sum_{t \in T} \overline{F}_t \tag{28}$$

Since the objective functions of the MILP and NLP are different, the MILP-NLP gap cannot be estimated for the solutions obtained with the process network model. Therefore, this MILP-

NLP method cannot guarantee that a feasible solution is within a certain gap of the global optimum. The motivation here is to generate a schedule (solution of binary variables) quickly that can guarantee the smelter is working at full capacity throughout the scheduling horizon. We then solve the NLP model to find a solution that maximizes the actual objective value, but the schedule obtained from the MILP might restrict the quality of the solution in reference to the original MINLP problem.

4.2.2. Multiple solutions in first MILP

In order to obtain better NLP solutions and avoid infeasible solutions, multiple solutions are generated in the first MILP stage. These solutions provide multiple schedules that can keep the smelter working at full capacity are generated. The MILP optimality gap for all solutions are set to 0. Then, a set of NLP problems are generated from all solutions in the MILP solution pool. Theoretically, we can collect a sufficiently large number of multiple solutions (>10000) and try to find the best solution in the NLP model. But this would require a large computational effort. Therefore, we collect 15 multiple solutions with the purpose of reducing the computational time. Inevitably, the solutions might be symmetric or similar to each other. GAMS provides a function for CPLEX to create a solution pool[34] that generates and keeps multiple solutions; a description of how to set up the corresponding parameters is presented in the Supporting Information.

5. Examples

5.1. Motivating example

We present a small motivating example to provide some insight on the complexity of this raw material blending problem. The instance consists of 2 vessels, 4 piles with initial inventories at the port, 1 pre-blender, 2 transfer ships, 1 non-concentrate material, 4 bins (8 sub-bins) and 1 smelter. Figure 2 shows a schematic representation of the motivating example.

The data for the for the motivating example represented in Figure 4 is given in Table S1 in the Supporting Information. The scheduling horizon is composed of 13 days and two marine vessels are scheduled to arrive at the beginning of day 1 (t=0) and day 7 (t = 6); they contain 11,380 and 10,800 tons of concentrates, respectively. Together with 3 piles of concentrates already present at the port, they can be mixed in the pre-blender. Two transfer ships transport material from the pre-blender to the production facility. There is one non-concentrate arriving on a daily basis to the production facility. The smelter is operated at full capacity, 1500 tons/time period. The properties that are being tracked are the mass fraction of four key components (K1-K4). There is a positive gross margin for every concentrate, but none for the non-concentrate materials. The transfer flowrates for the operations at the port are unlimited. In addition, the interdependency constraints and penalties for variation in concentration are not considered in the motivating example. The objective is to maximize the gross margin for processing raw materials during the scheduling horizon.

5.2. Industrial problem

We provide an industrial problem which is significantly larger than the motivating example. The problem consists of 5 vessels, 6 piles with initial inventories at the port, 1 pre-blender, 2 transfer ships, 3 non-concentrate materials, 6 bins (12 sub-bins) and 1 smelter. Interdependency constraints and penalties for variation in concentration of one key component are also considered. The duration of each time period is 0.5 days. Figure 9 shows a schematic representation of the industrial problem. The complete problem data is given in Table S2 in the Supporting Information.

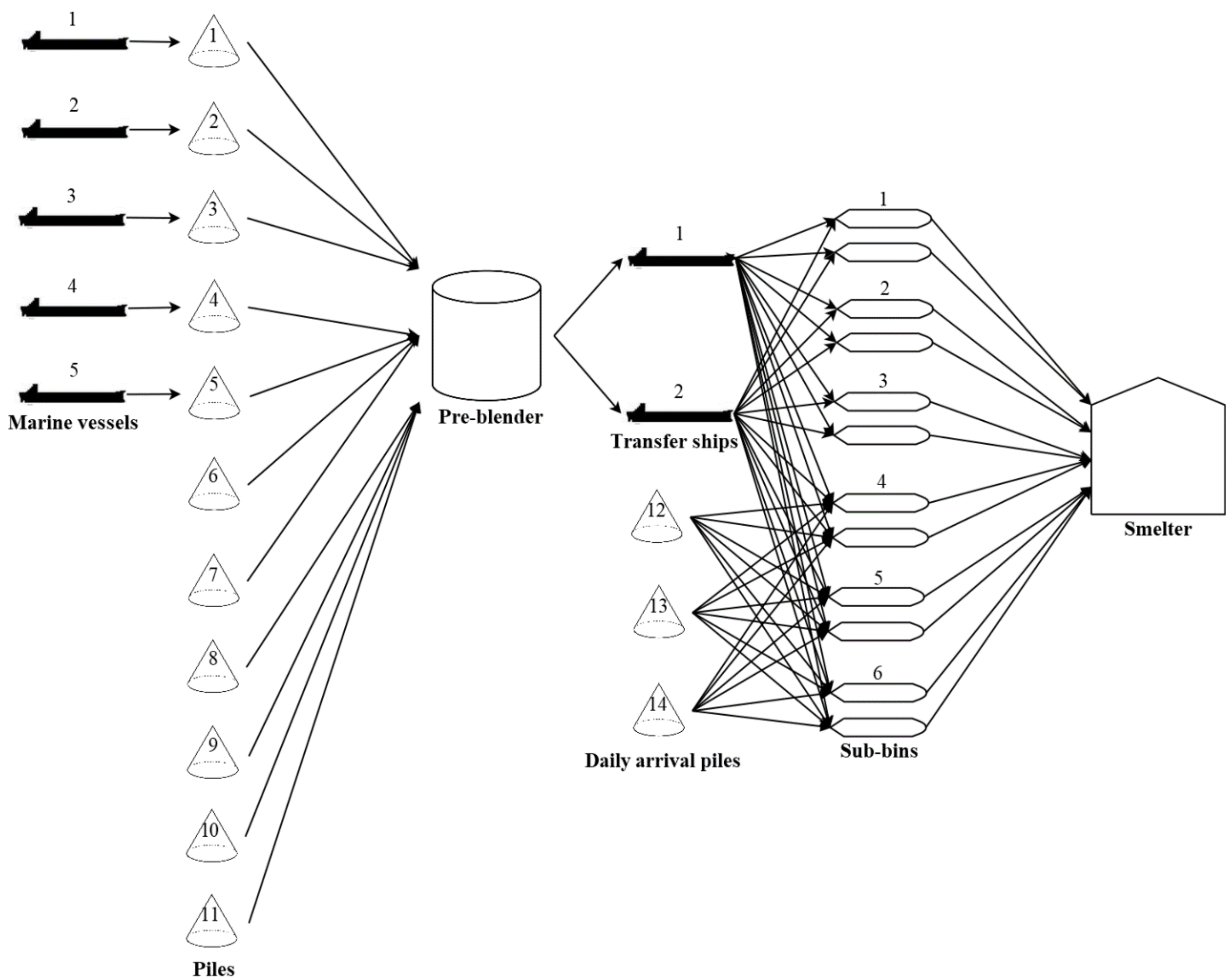

Figure 9. Schematic representation of the mixing network of the industrial problem.

6. Computational results

In this section, we address the raw material blend scheduling problem for the small motivating example and the industrial problem. For each of them, we compare the performance of the two formulations, the split fraction model and process network model. Therefore, we have 4 models to solve: 1) motivating example in split fraction model; 2) motivating example in process network model; 3) industrial problem in split fraction model; 4) industrial problem in process network model.

The differences between split fraction model and process network model, as shown in section 3, are mainly about: a) the mass balance equation, eq. 2a-2b and eq.4a-4d; b) the operations for non-concentrate materials, eq.12 and eq.13a-13b; c) the final blending, eq.21 and eq.22; d) the objective function, eq.25 and eq.26. We do not consider the interdependency constraints and penalties for the variation in concentration of the key components in the motivating example. Therefore, eq. 24a-24c and 27a-27b are excluded in the motivating example. The equations considered in each model are shown in Table 1.

Table 1. Equations of the four instances

Instance	Equations involved
Motivating example (SF)	(4)-(12),(14)-(21),(23),(25)
Motivating example (PN)	(2),(5)-(11),(13)-(20),(22),(23),(26)
Industrial problem (SF)	(4)-(12),(14)-(21),(23)-(25),(27)
Industrial problem (PN)	(2),(5)-(11),(13)-(20),(22),(23),(24),(26),(27)

We present the computational results of applying the solution strategy described in the previous section to the motivating example and industrial problem. The computational statistics of the instances are presented in Table 2. The algorithms and models were implemented in GAMS 24.7.1[35]. All computations were performed on a ASUS UX305 computer with two Intel Core i5 processors at 2.30 GHz and 2.40 GHz, 8 GB of RAM.

Table 2. The problems size of motivating and industrial instances

Model		Binary var.	Variables	Constraints
Motivating example (SF)	MILP	559	5,171	5,563
	NLP		5,171	7,435
Motivating example (PN)	MILP	559	1,850	3,096
	NLP		2,714	4,009
Industrial problem (SF)	MILP	2,490	45,253	47,404

	NLP		45,253	62,832
Industrial problem (PN)	MILP	2,490	12,090	12,963
	NLP		18,404	19,510

6.1. Motivating example (SF)

Table 3. Performance in the motivating example (SF)

Motivating example (SF)	MILP (CPLEX, gap = 2%)		NLP (CONOPT)		
MILP-NLP method	solution	CPU time	solution	CPU time	gap
	8.792	137 s	8.792	2 s	0%
	MINLP (BARON, gap = 2%)				
solved in a full space	solution		CPU time		
	8.793		3,007 s		

As shown in Table 3, after 140 s CPU time, the optimality gap is 0 between the solution of the MILP and the NLP, which means that the global optimum has been found. We also solve the full space MINLP model with BARON. A similar objective value is obtained but with a much longer CPU time, namely 3007 s. The slightly different objective values are because the MILP-NLP method and BARON converge to different MILP gap within 2%. Therefore, the solution by MILP-NLP method is applied for the following discussion.

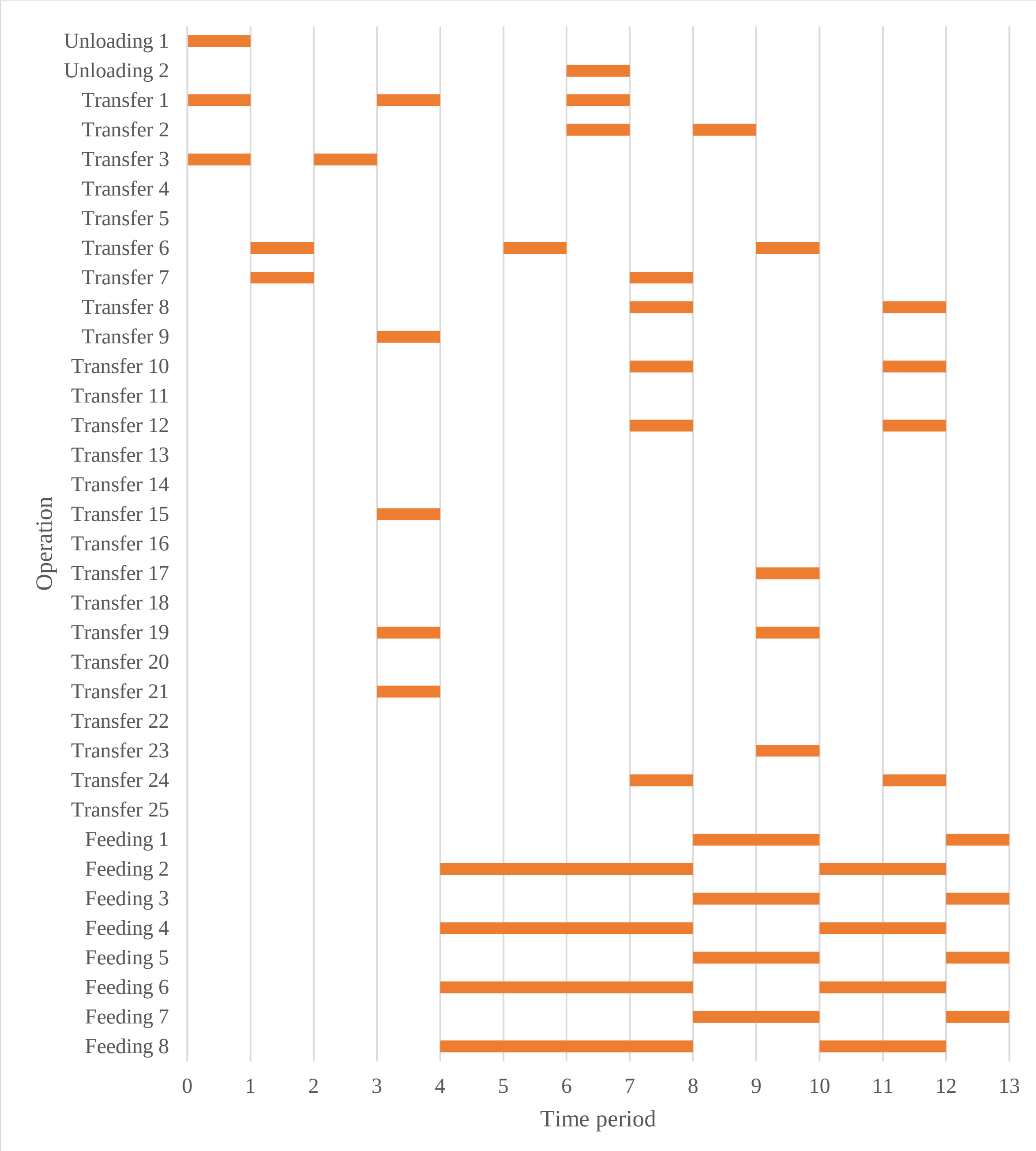

Figure 10. Gantt chart of optimal schedule for motivating example (profit: $8,792,740)

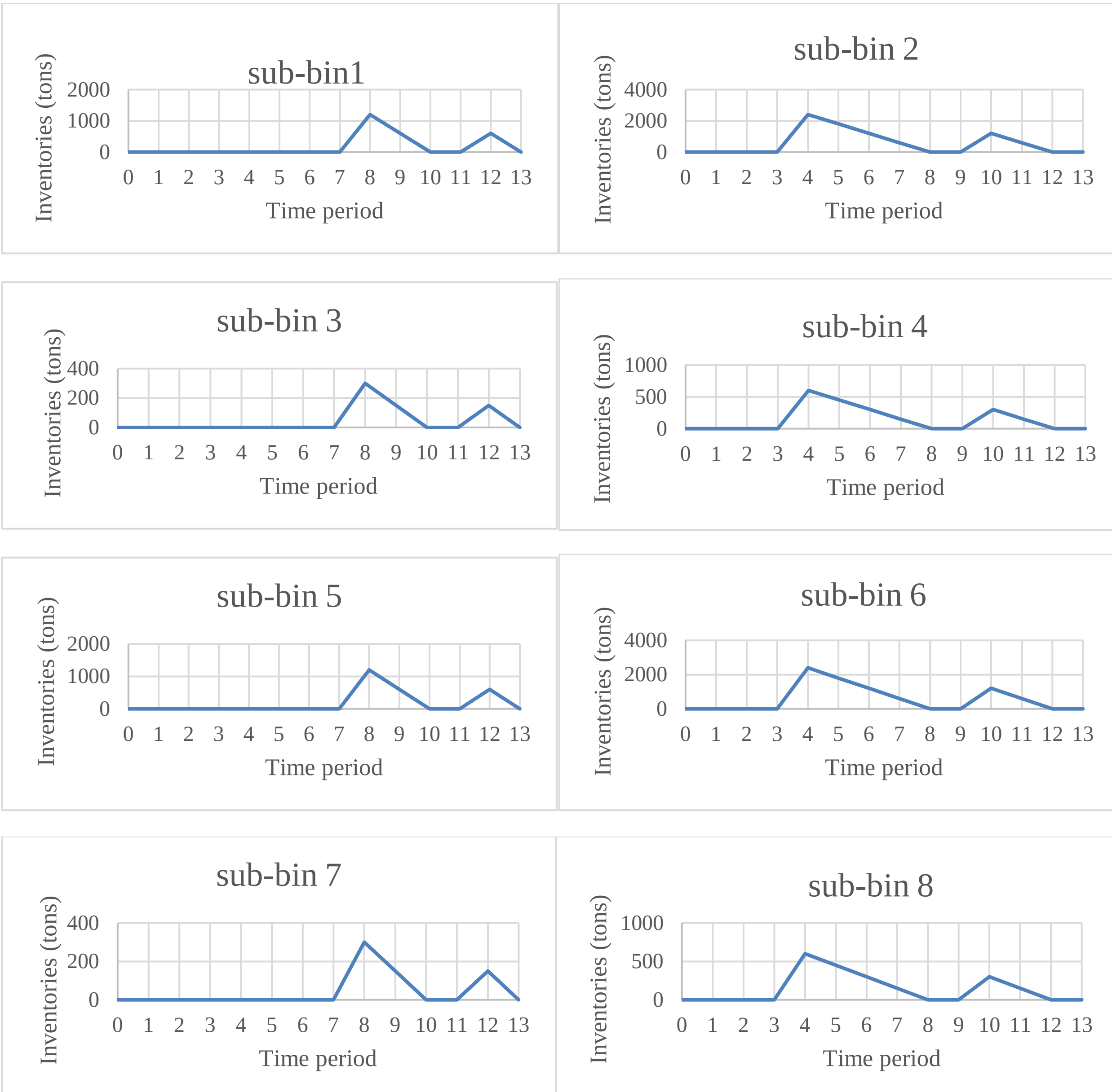

Figure 11. Inventories of sub-bins of the motivating example

Figure 10 depicts the Gantt Chart (see Table S3 for serial number of the operations) for the optimal solution of the motivating example with a profit of $8,792,740. Each task is represented by a horizontal bar and each row corresponds to a specific operation. The feeding operations 1-8 represent the discharging of sub-bins 1-8; we can observe that the first group of sub-bins (feeding 1,3,5,7) and the second group of sub-bins (feeding 2,4,6,8) work in cycles to keep the smelter operated continuously. From Figure 11, either the first group or the second group of sub-bins finish one feed recipe and becomes empty simultaneously, which physically means that the 8 bins use up to one mixture and start a new feed recipe simultaneously. In this case, there are 4 feeding recipes during the scheduling horizon which cover time periods 5-8, 9-10, 11-12, and 13.

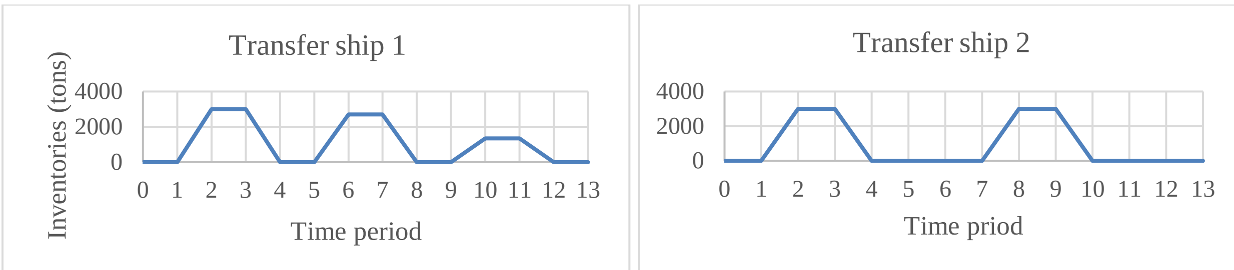

Figure 12. The inventories of transfer ships

From Figure 12, we can see the operation rule modeling the “transport delay” clearly apply for the transfer ships. The cycle time for loading, transporting, unloading, and returning is 4 time periods. Consider the first transfer operation of transfer ship 1 as an example. The ship is loading at time 2, transporting to the production facility at time 3, unloading material in at time 4, and returning to the port at time 5. The transfer ship 1 transfers materials three times during the scheduling horizon, which are at times 2-5, 6-9, 10-13. The transfer ship 2 transfers material two times at times2-5 and 8-11.

6.2. Motivating example (PN)

Table 4. Performance of the motivating example (PN)

Motivating example (PN) MILP-NLP decomposition	MILP (CPLEX, gap = 2%)				
	solution	CPU time	Number of alternative solutions		
	13,500*	6 s	15		
	NLP (CONOPT)				
Binary decisions	NLP solution	Binary decisions	NLP solution	Binary decisions	NLP solution
Schedule 1	7.980	Schedule 6	6.201	Schedule 11	4.809
Schedule 2	6.201	Schedule 7	6.201	Schedule 12	4.809
Schedule 3	6.201	Schedule 8	5.301	Schedule 13	4.809
Schedule 4	6.201	Schedule 9	5.601	Schedule 14	4.809
Schedule 5	6.201	Schedule 10	4.809	Schedule 15	6.201
	MINLP (BARON, gap = 2%)				
solved in a full space	lower bound			upper bound	CPU time
	7.960			8.832	15,000 s

* The objective value, 13,500 is equal to the total amount of processing materials when the smelter is operated at full capacity (i.e. 9×1,500).

We also applied the process network model for the motivating example. As mentioned in the previous section, the MINLP model is decomposed into MILP and NLP subproblems. The first MILP whose objective function is to maximize the total flowrate into the smelter is solved by CPLEX to generate multiple solutions. Then, the different binary decisions are fixed to solve the second NLP. The best objective value of NLP is selected.

As shown in Table 2, the model size of the process network model is smaller than the split fraction model, which is because in a process network model there are no variables for individual flows and inventories of components but their concentrations instead. On the other hand, the non-linearity of the NLP in the process network model is higher than the split fraction model.

Due to the large number of non-linearities, the motivating example (PN) cannot be solved by BARON in reasonable time. The proposed MILP-NLP decomposition method requires less computational effort. As shown in Table 4, 15 different binary decisions are generated from the first MILP model with an objective value equal to 13,500, which is the total amount of materials processed when the smelter is operated at full capacity (i.e. 9×1,500). Correspondingly, 15 NLP models are solved. There are only 6 different objective values out of 15 schedules, which is caused by neighboring schedules that are very similar to each other and lead to the same NLP solution. In this case, we select the solution based on schedule 1 as the final solution of the motivating example (PN); this solution yields an objective function value of 7,980. Note that this objective value is lower than the objective value of 8,792 obtained in the (SF) model.

6.3. Industrial problem (SF)

Table 5. Performance of the industrial problem (SF)

Industrial problem (SF)	MILP (CPLEX, gap = 1%), Rolling horizon with overlap				
The number of time periods in overlaps	The number of time periods in detailed time blocks				
	2	3	4	5	6
1	Infes (sub 4)	Infes (sub 2)	Infes (sub 2)	Infes (sub 2)	Infes (sub 2)
2		Infes (sub 3)	Infes (sub 2)	Infes (sub 3)	Infes (sub 2)
3			15.884 (1,114 s)	15.972 (705s)	15.860 (932s)
4				15.884 (2,094s)	16.050 (1,088s)
5					>2,500s

(3,5)	NLP (CONOPT4) solution	CPU time	MILP-NLP gap
	15.972	42s	0%

We try different combinations of the length of the detailed time block from 2-6, and the length of overlap from 1-5 to find the best solution with relatively less computational effort for a general solution process. Here, (3,5) means the combination of 3 time periods in overlap and 5 time periods in detailed time block. In Table 5, if the problem is feasible, the objective value and CPU time are displayed. Under the same length of the detailed time block, the required computational effort is larger as the overlap becomes longer. The (5,6) case does not return a solution after 2,500 seconds. Feasible solutions are available for the combinations (3,4), (3,5), (3,6), (4,5), and (4,6). Considering that all the objective values are close to each other and the CPU time of strategy (3,5) is 705s, which is the shortest, we select the binary decisions of (3,5) for the second NLP. It takes 42 seconds for the NLP model to return the same objective value obtained with in the MILP; the optimal objective value equals 15.972. Note that even if the MILP-NLP gap is 0 in this case, global optimality cannot be guaranteed since the MILP is solved by a rolling horizon strategy.

6.4. Industrial problem (PN)

Table 6. Performance of the industrial problem (PN)

Motivating example (PN)	MILP (CPLEX, gap = 2%)		
MILP-NLP decomposition	solution	CPU time	Number of alternative solutions
	39,000*	221 s	15

	NLP (CONOPT)				
Binary decisions	NLP solution	Binary decisions	NLP solution	Binary decisions	NLP solution
Schedule 1	Infes	Schedule 6	Infes	Schedule 11	Infes
Schedule 2	1.314 (7s)	Schedule 7	Infes	Schedule 12	Infes
Schedule 3	Infes	Schedule 8	Infes	Schedule 13	Infes
Schedule 4	Infes	Schedule 9	Infes	Schedule 14	Infes
Schedule 5	Infes	Schedule 10	-10.995 (25s)	Schedule 15	1.314 (6s)

* The objective value, 39,000 is equal to the total amount of processing materials when the smelter is operated at full capacity (i.e. $26 \times 1{,}500$).

For the process network model, we applied to the industrial problem (PN) the same procedure used in motivating example (PN). From Table 6, only 3 binary decisions lead to a feasible solution in the second NLP. The reasons are first, neighboring schedules that are very similar to each other are infeasible; second, for the industrial problem, the MILP relaxation ignores all composition equations, and therefore, the NLP with the quality constraints is infeasible; third, the MILP relaxation does not generate starting points of the composition information for the second NLP, and therefore, the poor starting point may lead to an infeasible solution. We select the solution based on schedule 15 with an objective value of 1,314 as a final solution of industrial problem (PN).

6.5. Variation in concentration of the key component

We consider the penalties of variation in concentration of the key component in the industrial problem.

Table 7. Economic data of the final solution of the industrial problem

Industrial problem	Objective value	Gross margin	Penalties for variation in concentration
SF	15.972	15.972	0
PN	1.314	13.751	12.394

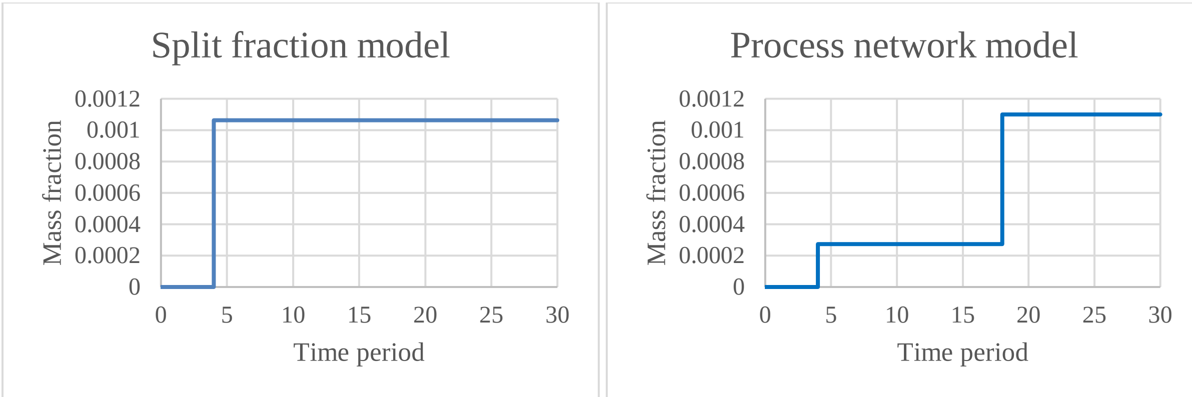

Figure 13. The mass fraction of K3 in the industrial problem

As seen in Table 7, the process network model returns a solution with lower gross margin and higher penalties. Also, one may notice that the solution of schedule 10 in Table 7 has a negative value which means the penalties are higher than the gross margin. However, the split fraction model can return an optimal solution without any penalties. The reason is that in the split fraction model, the penalties can be considered in the first MILP relaxation. But in the process network model, all composition information is ignored, and we only get binary decisions that can keep the smelter operated at full capacity. As a result, large penalties are generated in the second NLP model as shown in Figure 13. As mentioned in the problem statement section, the weight of penalties of variation in concentration of K3 is set to 100. In industrial analysis, one can reset the weight of penalties to obtain solutions with special requirement for the variation of key components' concentration.

7. Conclusion

The scheduling and feed quality optimization for processing raw materials in a copper smelter with two blending steps has been addressed in this paper. It was shown that this problem has some similarities with the crude oil scheduling problem. Special operation rules, such as *transport delay* and *shut down when empty* for operations in single time period and multiple time periods have been successfully modeled. Penalties for variations in concentration and linear constraints are considered in the objective function. Solution strategies, such as MILP-NLP decomposition method, relax-and-fix rolling horizon with nearby time window overlaps, and multiple solutions for MILP were applied to solve the large scale non-convex MINLP model.

Two formulations, process network model and split fraction model, were applied to this scheduling problem and the performances are contrasted as follows.

The split fraction model provides a tight MILP relaxation so that the optimality gap is close to 0. However, the model size is much larger and requires large computational effort since there are variables for individual flows and inventories. For the industrial problem, even the first MILP relaxation cannot be solved in the full space. Therefore, the relax-and-fix rolling horizon with nearby time window overlaps is applied. In summary, the split fraction model can be used to find better solutions with relatively larger computational efforts. Though global optimality cannot be guaranteed.

The process network model is smaller than the split fraction model, but with higher non-linearities, which cannot be solved in global MINLP solver in reasonable time. Once the nonlinear constraints are dropped, the MILP relaxation without any composition information can be solved in relatively less computational efforts. By generating multiple solutions in first MILP, we can find feasible and infeasible solutions for the NLP model, depending on the complexity of the problem. Since the objective functions of the MILP and NLP problems are different, it is not possible to estimate the optimality gap of its solutions. In summary, the process network model can be used to generate several feasible solutions faster without considering the optimality of the solutions.

ASSOCIATED CONTENT

Readers can find the data of the motivating example (Table S1) and industrial problem (Table S2), serial number of the operations for the motivating example (Table S3) and the parameters to set up solution pool from CPLEX (Table C1) in the supporting information.

AUTHOR INFORMATION

Corresponding Author

*E-mail: grossmann@cmu.edu

ACKNOWLEDGMENT

The authors are grateful to the Center for Advanced Process Decision-making at Carnegie Mellon University for their involvement in the collaboration project with the Research, Development & Innovation Department at Aurubis AG. The second author was funded by the Brazilian National Research Council (CNPq) under grant Ciências sem Fronteiras number 201542/2015-3.

NOMENCLATURE

Subscripts

t: time period

(n, i, o): intermediate unit

v: vessel

p: pile on the port

b: pre-blender

TS: transfer ship

dp: daily arrival pile

sb: sub-bin

s: smelter

c: concentrate

k: key component

Sets

T: time periods

N: intermediate units $N = P \cup B \cup TS \cup DP \cup SB$

O_n: The downstream units of unit *n*

I_n : The upstream units of unit *n*

V : vessels

P : piles on the port

B : pre-blender

TS : transfer ships

DP: daily arrival piles

SB: sub-bins $SB = FSB \cup SSB$

FSB: first group of sub-bins

SSB: second group of sub-bins

S : smelter

C : concentrates

DC : daily arrival concentrates

K : key components

Parameters

$[\underline{F_{n,o}}, \overline{F_{n,o}}]$: bounds on flow from intermediate unit *n* to *o*

$[\underline{M_n}, \overline{M_n}]$: bounds on inventories of intermediate unit *n*

M_n^0 : initial total inventories of intermediate unit *n*

$m_{n,c}^0$: initial inventories of concentrate *c* of intermediate unit *n*

$\theta_{k,c}$: mass fraction of component *k* in concentrate *c*

Ke_k : parameters for interdependency constraints of component *k*

Ue_k : parameters for interdependency constraints of component *k*

α_c : income for processing unit concentrate *c*

β_k : weight of flow change for key component *k*

$\widehat{F}_s$: the maximum operating capacity of the smelter *s*

χ_k : upper bound of mass fraction of key component *k* for the final blending

MD : maximum amount of non-concentrates material at the end of scheduling horizon

TMH : the length of scheduling horizon

ET : the earliest time period when smelter is operated

$F_{v,p,t}$: the flowrate from vessel *v* to pile *p* at time *t*

Variables

Binary variables

$D_{n,o,t}$: variables that indicates the existence of flow from intermediate unit *n* to *o* at time *t*

Df_t : variables that indicate if the first group of sun-bins are feeding the smelter at time *t*

$D\hat{f}_t$: variable that indicate if the first group of sub-bins finish feeding recipe at time *t*

Ds_t : variables that indicate if the second group of sub-bins are feeding the smelter at time *t*

$D\hat{s}_t$: variables that indicate if the second group of sub-bins finish feeding recipe at time *t*

$X_{n,t}$: variables that indicate if the intermediate unit *n* is discharged at time *t*

$E_{n,t}$: variables that indicate if there are materials in the intermediate unit *n* at time *t*

Continuous variables

$F_{n,o,t}$: total flowrate from intermediate unit *n* to n' at time *t*

$f_{n,o,c,t}$: flowrate of concentrate *c* from intermediate unit *n* to n' at time *t*

$M_{n,t}$: total inventories of intermediate unit *n* at time *t*

$m_{n,c,t}$: inventories of concentrate *c* of intermediate unit *n* at time *t*

$x_{n,c,t}$: mass fraction of concentrate *c* in intermediate unit *n* at time *t*

$\tilde{F}_{k,t}$: flowrate of key component *k* into the smelter at time *t*

$\overline{F}_t$: total flowrate into the smelter at time t

$Z_{k,t}$: flowrate change of key component k in final mixture at time t

REFERENCES

(1) Langner, B. E. Understanding copper: Technologies, markets, business. Eigenverl. **2011**.

(2) Copper Alliance. The electric vehicle market and copper demand. **2017**. Retrieved from http://copperalliance.org/trends/the-electric-vehicle-market-and-copper-demand/.

(3) European Copper Institute. Is there enough copper from the energy transition? **2017**. Retrieved from http://copperalliance.eu/news-and-media/news-articles/is-there-enough-copper-for-the-energy-transition-.

(4) Lee, H.; Pinto, J. M.; Grossmann, I. E.; Park, S. Mixed-integer linear programming model for refinery short-term scheduling of crude oil unloading with inventory management. *Ind. Eng.* Chem. Res., **1996**, 35 (5), 1630-1641.

(5) Mendez, C. A.; Grossmann, I. E.; Harjunkoski, I.; Kabore, P. A simultaneous optimization approach for off-line blending and scheduling of oil-refinery operations. *Comput. Chem. Eng.*, **2006**, 30, 614–634.

(6) Mouret, S.; Grossmann, I. E.; Pestiaux, P. A novel priority-slot based continuous-time formulation for crude-oil scheduling problems. *Ind. Eng. Chem. Res.*, **2009**, 48 (18), 8515-8528.

(7) Castro, P.; Grossmann, I. E. Global optimal scheduling of crude oil blending operations with RTN continuous-time and multiparametric disaggregation. *Ind. Eng. Chem. Res.*, **2014**, 53 (39), 15127-15145.

(8) Cerda, J.; Pautasso, P. C.; Cafaro, D. C. Efficient approach for scheduling crude oil operations in marine-access refineries. *Ind. Eng. Chem. Res.*, **2015**, 54 (33), 8219-8238.

(9) Cerda, J.; Pautasso, P. C.; Cafaro, D. C. A cost-effective model for the gasoline blend optimization problem. *AIChE J*., **2016**, 62 (9), 3002-3019.

(10) Cerda, J.; Pautasso, P. C.; Cafaro, D. C. Optimizing gasoline recipes and blending operations using nonlinear blend models. *Ind. Eng. Chem. Res.*, **2016**, 55 (28), 7782-7800.

(11) Kelly, J. D.; Menezes, B. C.; Engineer, F.; Grossmann, I. E. Crude-oil blend scheduling optimization of an industrial-sized refinery: a discrete-time benchmark. In Foundations of Computer Aided Process Operations, **2017**: Tucson, United States.

(12) McCormick, G. P. Computability of global solutions to factorable nonconvex programs: Part 1- convex underestimating problems. *Math. Program*., **1976**, 10 (1), 147-175.

(13) Al-Khayyal, F. A.; Falk, J. E. Jointly constrained biconvex programming. *Math. of Oper. Res.*, **1983**, 8 (2), 273-286.

(14) Andrade, T.; Ribas, G.; Oliveira, F. A strategy based on convex relaxation for solving the oil refinery operations planning problem. In Foundations of Computer Aided Process Operations, **2017**: Tucson, United States.

(15) Assis, L. S.; Camponogara, E.; Zimberg, B.; Ferreira, E.; Grossmann, I. E. A piecewise McCormick relaxation-based strategy for scheduling operations in a crude oil terminal. *Comput. Chem. Eng.*, **2017**, 106 (2), 309-321.

(16) Menezes, B. C.; Kelly, J. D.; Grossmann, I. E. LP Reformulation to Approximate Non-Convex Blending in MILP Scheduling Optimization using Factors for Qualities. In AICHE Annual Meeting, **2017**: Minneapolis, United States.

(17) Jia, Z.; Ierapetritou, M.; Kelly, J. D. Refinery short-term scheduling using continuous time formulation: crude-oil operations. *Ind. Eng. Chem. Res*., **2003**, 42 (13), 3085.

(18) Mouret, S.; Grossmann, I. E.; Pestiaux, P. Time representations and mathematical models for process scheduling problems. *Comput. Chem. Eng*., **2011**, 35 (6), 1038-1063.

(19) Joly, M.; Pinto, J. M. Mixed-integer programming techniques for the scheduling of fuel oil

and asphalt production. *Chem. Eng. Res. Des.*, **2003**, 81 (4), 427-447.

(20) Floudas, C. A.; Lin, X. Continuous-time versus discrete-time approaches for scheduling of chemical processes: a review. *Comput. Chem. Eng.,* **2004**, 28 (11), 2109-2129.

(21) Geoffrion A. Generalized Benders Decomposition. *J. Optim. Theory App.*, **1972**, 10, 237-260.

(22) Guignard, M.; Kim, S. Lagrangean decomposition: a model yielding stronger Lagrangean bounds. *Math. Program.*, **1987**, 39, 215–228.

(23) Zamarripa, M.; Marchetti, P. A.; Grossmann, I. E.; Singh, T.; Lotero, I.; Gopalakrishnan, A.; Besancon, B.; Andre, J. Rolling Horizon Approach for Production-Distribution Coordination of Industrial Gases Supply Chains. *Ind. Eng. Chem. Res.*, **2016**, 5 (9), 2646-2660.

(24) Kelly, J. D. Chronological decomposition heuristic for scheduling: Divide and conquer method. *AIChE J*., **2002**, 48(12), 2995-2999.

(25) Lee, H.; Maravelias, C.T. Combining the strengths of continuous and discrete time representations: a general solution refinement method for discrete-time MIP models, presented at the 2017 AIChE Annual Meeting, Minneapolis, MN, US (Oct. 29-Nov. 2, **2017**).

(26) Misener, R.; Floudas, C. A. Advances for the pooling problem: modeling, global optimization, and computational studies. *Appl. Comput. Math.*, **2009**, 8 (1), 3-22.

(27) Haverly, C. A. Studies of the behavior of recursion for the pooling problem. Acm sigmap bulletin, **1978**, 25, 19-28.

(28) Ben-Tal, A.; Eiger, G.; Gershovitz, V. Global minimization by reducing the duality gap. *Math. Prog.*, **1994**, 63 (1), 193-212.

(29) Alfaki, M.; Haugland, D. Strong formulations for the pooling problem. *J. Glob. Optim.*, **2013**, 1-20.

(30) Sahinidis, N. V; Tawarmalani, M. Accelerating branch-and-bound through a modeling language construct for relaxation-specific constraints. *J. Glob. Optim.*, **2005**, 32 (2), 259-280.

(31) Lotero, I.; Trespalacios, F.; Grossmann, I. E.; Papageorgiou, D. J.; Cheon, M. S. An MILP-MINLP decomposition method for the global optimization of a source-based model of the multiperiod blending problem. *Comput. Chem. Eng.*, **2016**, 87 (6), 13-35.

(32) Quesada, I.; Grossmann, I. E. Global optimization of bilinear process networks with multicomponent flows. *Comput. Chem. Eng.*, **1995**, 9 (12), 1219-1242.

(33) Zyngier, D., Kelly, J. D.. Multi-product Inventory Logistics Modeling in The Process Industries. In: Wanpracha Chaovalitwongse, Kevin C. Furman, Panos M. Pardalos (Eds.) Optimization and logistics challenges in the enterprise. Springer optimization and its applications, **2009**, 30, Part 1, 61.

(34) GAMS Development Corporation, Washington, DC, USA. GAMS - The Solver Manuals, GAMS Release 24.7.1, **2016**.

(35) GAMS Development Corporation. General Algebraic Modeling System (GAMS) Release 24.7.1. Washington, DC, USA, **2016**.

Table of Contents